Available online at www.sciencedirect.com
ScienceDirect
Journal of Molecular Catalysis A: Chemical 258 (2006) 313–319
JOURNAL OF MOLECULAR CATALYSIS A: CHEMICAL
www.elsevier.com/locate/molcata

# Dispersion and reactivity of monolayer vanadium oxide catalysts supported on zirconia: The influence of molybdena addition

Komandur V.R. Chary *, Chinthala Praveen Kumar, Taduri Rajiah, Chakravartula S. Srikanth

*Catalysis Division, Indian Institute of Chemical Technology, Hyderabad 500 007, India*

Received 20 August 2005; received in revised form 19 May 2006; accepted 22 May 2006
Available online 10 July 2006

**Abstract**

This investigation reports the influence of $MoO_3$ on the dispersion of vanadium oxide on zirconia support. Samples containing various $MoO_3$ loadings ranging from 0.5 to 4 wt.% were prepared by impregnation of previously prepared 6 wt.% $V_2O_5/ZrO_2$ with requisite amounts of ammonium heptamolybdate solution. Dispersion of vanadia was determined by oxygen chemisorption at 640 K and was found to decrease with the increase of molybdena loading. The calcined catalyst samples were characterized by specific BET surface area, XRD, FT-IR, Oxygen chemisorption and TPR of $H_2$ techniques. The XRD results show that the intensity of tetragonal phase decreases and monoclinic phase intensity increases with the addition of $MoO_3$ to $V_2O_5/ZrO_2$ catalyst. The TPR of $H_2$ results reveal that the reducibility of vanadia was found to decrease with the addition of molybdena to $V_2O_5/ZrO_2$ catalyst. The catalytic properties were evaluated during the ammoxidation of 3-picoline to nicotinonitrile. The activity in ammoxidation reaction did not change much with the addition of molybdenum oxide. However, the selectivity of nicotinonitrile was found to increase with molybdena loading, indicates that the added molybdena created additional sites for the ammoxidation of 3-picoline reaction. The addition of molybdenum oxide inhibited the interaction between vanadium and zirconia, leading to decrease in dispersion and reducibility of vanadia.


*Keywords:* Vanadia–molybdena; Zirconia; Dispersion; Ammoxidation

## 1. Introduction

Vanadium oxides form a group of industrially important catalysts for the ammoxidation and partial oxidation of aromatic hydrocarbons as well as for NO reduction with $NH_3$ [1–5]. Much research activity has been devoted towards understanding the nature of active sites as well as the role played by the catalyst support. The most efficient utilization of any supported catalyst depends on the percent exposed or the dispersion of the active component on the surface of the support. The dispersion is often controlled, among other factors, by the extent of loading and the nature of the support. The active component may remain as a highly dispersed monolayer or as crystallites on the support surface, or it may even form a solid solution with the latter [6,7]. In the recent past, zirconia has been investigated as a potential catalyst support [8–11]. It is also been employed in many industrially important reactions such as hydroprocessing [8,9], oxidation of alcohols [12,13] and synthesis of methanol and higher alcohols [14,15]. The advantages of using zirconia as a catalyst support includes (i) it interacts strongly with the active phase; (ii) it possesses high thermal stability and is more chemically inert than the classical oxides; (iii) it is the only metal oxide which may possess all four chemical properties: namely acidity, basicity, reducing ability and oxidizing ability; (iv) it exhibit super-acidic properties when modified with small quantities of sulfate ions.

Many aspects of vanadia catalysts like method of preparation, kinetics and mechanism of the reactions, the effect of supports, the influence of promoters and the role of the V=O bond have been extensively investigated. Traditionally, oxides of several elements such as Nb, Sb, P, K, Na, Cs, Rb, Mo, and W have been used as additives to supported vanadia catalysts in order to increase their activity and to improve their selectivity for oxidation reactions [16,17]. Molybdenum is frequently added as a promoter to vanadium-based catalysts for a number of selective oxidations [18–20]. For example, $V_2O_5$ in com-

* Corresponding author. Tel.: +91 40 27193162; fax: +91 40 27160921.
*E-mail address:* kvrchary@iict.res.in (K.V.R. Chary).

1381-1169/$ – see front matter © 2006 Elsevier B.V. All rights reserved.
doi:10.1016/j.molcata.2006.05.049

bination with $MoO_3$ was employed in selective oxidation of benzene to maleic anhydride and *o*-xylene to phthalic anhydride [21]. Dejoz et al. [22] reported the role of molybdenum in Mo doped V–Mg–O catalysts during oxidative dehydrogenation of *n*-butane and suggested that the incorporation of $MoO_3$ favors oxydehydrogenated products more than undoped samples.

In view of the potential use of zirconia as a catalyst support and Mo as a promoter, in the present work a systematic investigation has been undertaken to investigate the dispersion and reactivity of $MoO_3$–$V_2O_5/ZrO_2$ catalysts. The influence of the presence of molybdenum oxide on the dispersion of vanadium and also on the catalytic activity during the ammoxidation of 3-picoline to nicotinonitrile has been discussed.

## 2. Experimental

Zirconia support was prepared by ammonical hydrolysis of zirconium oxychloride (Fluka) at pH 9, followed by calcination in air at 773 K for 6 h. The $MoO_3$–$V_2O_5/ZrO_2$ catalysts prepared by wet impregnation method and it involves two steps. In first step, 6 wt.% $V_2O_5$ supported on $ZrO_2$ was prepared by wet impregnation of the support using an aqueous solution containing ammonium metavanadate ($NH_4VO_3$). After impregnation, the sample was dried at 383 K and calcined in air at 773 K for 6 h. In the second step a series of $V_2O_5$–$MoO_3/ZrO_2$ catalysts with varying $MoO_3$ content ranging from 0.5 to 4 wt.% prepared by wet impregnation of previously prepared and oven dried 6% $V_2O_5/ZrO_2$ catalyst using stoichiometric amounts of an aqueous solution containing ammonium heptamolybdate. The samples were dried at 383 K for 16 h and further calcined at 773 K for 6 h in air.

A conventional all glass high vacuum system was used to determine the surface area by nitrogen adsorption at liquid nitrogen temperature (77 K). Oxygen chemisorption was measured by a static method using a Pyrex glass system capable of attaining a vacuum of $10^{-6}$ Torr. The details of the experimental set up were given elsewhere [23]. Prior to adsorption measurements the samples were pre-reduced in a flow of hydrogen (40 ml/min) at 640 K for 2 h and evacuated at the same temperature for an hour. Oxygen chemisorption uptakes were determined as the difference of two successive adsorption isotherms measured at 640 K.

Fourier transform infrared spectra of the samples were recorded on Nicolet 740 FT-IR spectrometer at ambient conditions by using KBr.

TPR of $H_2$ studies of the present catalyst samples were conducted on Auto Chem 2910 (Micromeritics, USA) instrument. The unit has a programmable furnace with a maximum operating temperature of 1373 K. The instrument was interfaced with a computer which performs tasks such as programmed heating and cooling cycles, continuous data recording, gas valve switching, data storage and analysis.

In a typical experiment for the TPR about 250 mg of oven dried sample (dried at 383 K for 12 h) was taken in a U-shaped quartz cell. The catalyst was packed in between two quartz wool plugs in one arm of the sample tube. The temperature was monitored with the aid of thermocouple located near the sample. The gas flows were monitored by highly sensitive mass flow controllers (Brooks). Prior to TPR studies the catalyst sample was pretreated in He flow (50 ml/min) at 673 K for 2 h. After pretreatment the sample was cooled to ambient temperature. Now the TPR analysis was carried out in reducing mixture (50 ml/min) consisting of 5% $H_2$ and balance Ar from ambient temperature to 1273 K at a heating rate of 5 K/min. The reducing gas was purified by passing through oxy-trap and molecular sieves to remove oxygen and any moisture from the reducing mixture. The hydrogen concentration in the effluent stream was monitored with the thermal conductivity detector (TCD) and the $H_2$ consumption values were calculated by calibration experiments using GRAMS/32 software. Calibration of the TCD was performed by stoichiometric reduction of a known amount of high purity $Ag_2O$ to Ag, a method, which was found to be more reliable and reproducible.

A down flow fixed bed reactor operating at atmospheric pressure and made of Pyrex glass was used to test the catalytic performance of the catalysts during the ammoxidation of 3-picoline to nicotinonitrile. About 2 g of the catalyst with a 18–25 mesh size diluted with an equal amount of quartz grains of the same dimensions was charged into the reactor supported on a glass wool bed. In order to minimize the adverse thermal effects, the catalyst particles were diluted to its same volume with quartz grains of similar particle size. Prior to introducing the reactant, i.e., 3-picoline with a syringe pump the catalyst was pre-reduced at 673 K for 2 h in purified hydrogen flow (40 ml/min). After the pre-reduction, the reactor was fed with 3-picoline, ammonia and air, keeping the mole ratio of 3-picoline: $H_2O$: $NH_3$: air at 1:13:22:44 and contact time at 0.6 s. The reaction was carried out at a temperature of 640 K. The liquid products nicotinonitrile and pyridine were analyzed by the gas chromatography (HP-6890) equipped with flame ionization detector (FID) using HP-5 capillary column.

## 3. Discussion

$ZrO_2$ exists in three crystallographic polymorphs viz., monoclinic, tetragonal and cubic [24]. The X-ray diffraction patterns of 6 wt.% $V_2O_5/ZrO_2$ and various $MoO_3$–$V_2O_5/ZrO_2$ catalysts are shown in Fig. 1. The synthesized zirconia was found to show the presence of monoclinic phase and tetragonal phases. The intense sharp reflections at $d = 3.16$ and 2.84 Å ($2\theta = 28.2°$ and 31.5°) are due to the monoclinic form of zirconia and the reflections at $d = 2.96$ and 1.83 Å ($2\theta = 30.16°$ and 49.8°) are due to tetragonal form of zirconia. These zirconia diffraction peaks can be seen in all the catalyst samples. A mixed vanadium and zirconium such as $ZrV_2O_7$ was formed due to the interactions between vanadia and zirconia in 6 wt.% $V_2O_5/ZrO_2$ catalyst (Fig. 1(a)) in addition to tetragonal and monoclinic phases of zirconia. The reflections due to $ZrV_2O_7$ can be seen at $d = 2.642$ Å ($2\theta = 33.9°$, JCPDS file no. 16-422) in all the catalyst samples. The intensity of $ZrV_2O_7$ phase was found to increase slightly with increase in molybdena loading from 0.5 to 4 wt.%. The addition of $MoO_3$ brings a dramatic reversal of intensities corresponding to the monoclinic and tetragonal reflections (Fig. 1(b)–(e)). The intensity of tetragonal zirconia

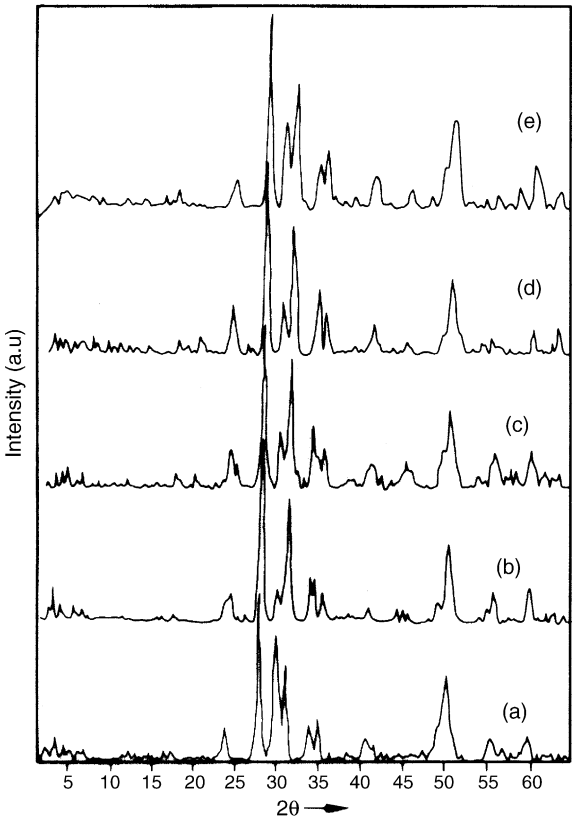


Fig. 1. X-ray diffraction pattern of various $MoO_3$–$V_2O_5/ZrO_2$ catalysts: (a) 6 wt.% $V_2O_5/ZrO_2$; (b) 0.5% Mo–$V_2O_5/ZrO_2$; (c) 2% Mo–$V_2O_5/ZrO_2$; (d) 3% Mo–$V_2O_5/ZrO_2$; (e) 4% Mo–$V_2O_5/ZrO_2$.

phase at $2\theta = 30.16^\circ$ is found to decrease drastically and the intensity of monoclinic zirconia phase at $2\theta = 31.5^\circ$ is increased with molybdena loading. This might be due to the specific interactions between vanadia and zirconia.

The BET specific surface areas of the $MoO_3$–$V_2O_5/ZrO_2$ catalysts are given in Table 1. The specific surface area of pure zirconia is found to be 84 $m^2/g$. The surface area was decreased in 6 wt.% $V_2O_5/ZrO_2$ catalyst which is attributed to the pore blockage of the support surface by crystallites of vanadia. With the addition of molybdena the surface area did not change much at lower loadings and decreased slightly with further increase in molybdena loadings. Oxygen chemisorption measurements were performed by a static method to determine the dispersion of vanadium oxide on zirconia support. As described by Oyama et al. [25], the pre-reduction of the sample and subsequent

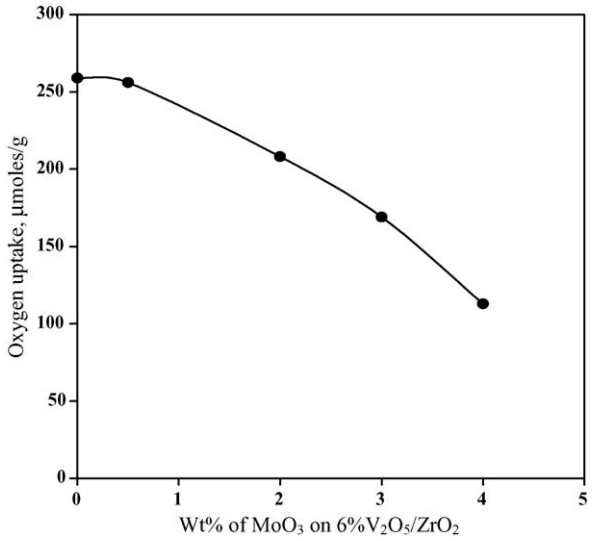


Fig. 2. Oxygen uptake plotted as a function of $MoO_3$ loading on 6% $V_2O_5/ZrO_2$ ($T_{ads} = T_{red} = 640$ K).

oxygen chemisorption were carried out at 640 K. Results of oxygen chemisorption by various $MoO_3$–$V_2O_5/ZrO_2$ catalysts were plotted as a function of Mo loading in Fig. 2. Fig. 2 shows that oxygen uptake at 640 K for various $MoO_3$–$V_2O_5/ZrO_2$ catalysts plotted as a function of Mo content. The amount of oxygen chemisorbed was calculated using the double isotherm method described by Parekh and Weller [26]. Pure $ZrO_2$ support did not chemisorb oxygen under the same experimental conditions, which are employed for the Mo–V supported catalysts. The $O_2$ uptakes along with surface area, oxygen atom site densities and dispersion values determined for various $MoO_3$–$V_2O_5/ZrO_2$ catalysts are shown in Table 1. It is clear that oxygen uptake decreases with increase of molybdena content in the catalysts. It is instructive to consider what can possibly happen to the added molybdena to the $V_2O_5/ZrO_2$ monolayer catalysts. Three possibilities can be conceived: (i) part of the added molybdena can interact with hydroxyl groups on zirconia left after vanadia impregnation, because it is well known that molybdena interacts with the hydroxyl groups on zirconia [27], (ii) the molybdena may cover part of the monolayer vanadia, (iii) the molybdena might interact with vanadia to form a surface compound which is difficult to reduce. Now let us consider the influence of the above possibilities on oxygen uptake by $MoO_3$–$V_2O_5/ZrO_2$ catalysts. According to the first possibility the oxygen chemisorption should increase as it is known that

Table 1
Oxygen uptake, dispersion, oxygen atom sites density and surface areas of $MoO_3$–$V_2O_5/ZrO_2$ catalysts

| Catalyst | Wt.% of $MoO_3$ | BET surface area ($m^2/g$) | Reduced BET surface area ($m^2/g$) | Oxygen uptake[a] (μmol/g) | Oxygen atom site density ($10^{18}/m^2$) | Dispersion[b] (O/V) |
|---|---|---|---|---|---|---|
| 6% VZr | 0 | 67 | 78 | 259 | 4.0 | 0.79 |
| 1MoVZr | 0.5 | 67 | 80 | 256 | 3.85 | 0.77 |
| 2MoVZr | 2 | 62 | 78 | 208 | 3.21 | 0.63 |
| 3MoVZr | 3 | 54 | 61 | 169 | 3.33 | 0.51 |
| 4MoVZr | 4 | 53 | 58 | 113 | 2.34 | 0.34 |

[a] $T_{(reduction)} = T_{(adsorption)} = 640$ K.
[b] Dispersion = fraction of vanadium atoms at the surface assuming $O_{ads}/V_{surf} = 1$.

the reduced molybdena on oxide support chemisorb oxygen [28]. It is experimentally found that oxygen chemisorption is decreasing with the addition of molydenum oxide on zirconia (Table 1). Therefore, the first possibility seems to be ruled out if the molybdena reduces, as does the vanadia. The second possibility predicts more or less constant oxygen chemisorption with the increase of molybdena, if the molybdena covering $V_2O_4$ units chemisorb oxygen, otherwise a decrease is visualized. The third possibility indicates a decrease in oxygen chemisorption since the surface compound formation is expected to decrease the dispersion of both the components. In reality all of the three possibilities may simultaneously occur to different extents. The decrease in oxygen chemisorption indicates that the third possibility is the most important one. However, one can not ruled out the possibility that a small fraction of molybdena interact with the hydroxyl groups of bare zirconia surface left out on the monolayer $V_2O_5/ZrO_2$. Because of this phenomenon the increase in oxygen chemisorption is expected to the small. Therefore, the net decrease in oxygen chemisorption led us to believe that the third possibility predominates in $MoO_3$–$V_2O_5/ZrO_2$ catalysts.

The FT-IR spectra of 6 wt.% $V_2O_5/ZrO_2$ and some of the $MoO_3$–$V_2O_5/ZrO_2$ catalysts are presented in Fig. 3. The characteristic bands due to $V_2O_5$ can be seen at 1020 and 825 $cm^{-1}$ corresponding to V=O stretching vibration and V–O–V deformation respectively [29,30]. The intensity of bands due to vanadia is found to decrease with the addition of molybdena. The characteristic bands for molybdena are at 1000 and 870 $cm^{-1}$ corresponding to Mo=O stretching vibration and Mo–O–Mo linkages [31]. The Mo–O–Mo linkage band at 870 $cm^{-1}$ can be seen in molybdena supported catalysts in Fig. 3(b)–(e). The

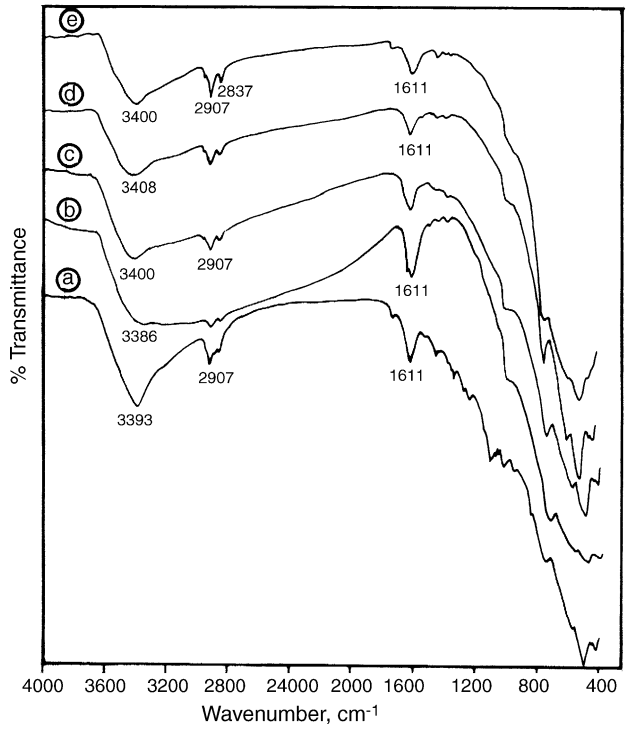


Fig. 3. FT-IR spectra of $MoO_3$–$V_2O_5/ZrO_2$ catalysts: (a) 6% $V_2O_5/ZrO_2$; (b) 0.5% $MoO_3$–$V_2O_5/ZrO_2$; (c) 2%; (d) 3%; (e) 4%.

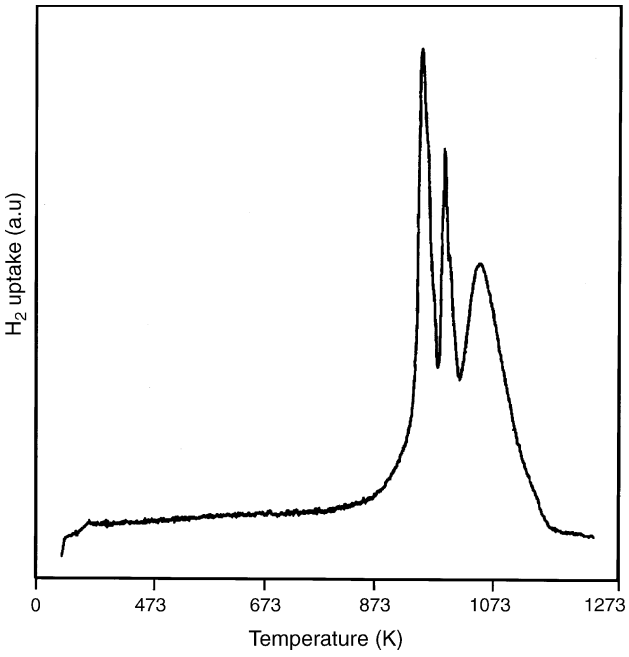


Fig. 4. Temperature-programmed reduction (TPR) profile of pure $V_2O_5$.

broad band at ~3400 $cm^{-1}$ is ascribed to surface hydroxyl groups and possibly due to $ZrO(OH)_2$. The intensities of the bands at ~1611 and ~3400 $cm^{-1}$ have decreased with increase in molybdena loading of the catalysts. Bond et al. [32] have attributed these bands to the deformation vibrations of adsorbed water and surface OH groups of the support. The decrease in the intensity of hydroxyl groups at 3400 $cm^{-1}$ might be due to the interactions between added molybdena hydroxyl groups present on the surface of the support.

The temperature-programmed reduction profile of unsupported $V_2O_5$ is shown in Fig. 4. The profile shows multiple major reduction peaks at 965, 1003, and 1067 K when treated in 5% $H_2$-in-Ar up to 1273 K. Koranne et al. [33] and Bosch et al. [34] have reported a similar observation, and they have attributed this phenomenon to the following reduction sequence:

$$V_2O_5 \rightarrow V_6O_{13} \quad (1)$$

$$V_6O_{13} \rightarrow V_2O_4 \quad (2)$$

$$V_2O_4 \rightarrow V_2O_3 \quad (3)$$

The sharp peak at 965 K corresponds to the reduction of $V_2O_5$ to $V_6O_{13}$ (first peak), the peak at 1003 K is associated with the reduction of $V_6O_{13}$ to $V_2O_4$ (second step), and the peak at 1067 K corresponds to $V_2O_3$ formed by the reduction of $V_2O_4$.

The TPR profile of unsupported $MoO_3$ has been presented in Fig. 5 and it shows two major peaks at 1040, 1270 K and one minor peak at 1070 K. According to Thomas et al. [35] and Arnoldy et al. [36], the reduction of molybdena essentially can take place in two steps. The following steps present in the reducibility of $MoO_3$:

$$MoO_3 \rightarrow MoO_2$$

$$MoO_2 \rightarrow Mo$$

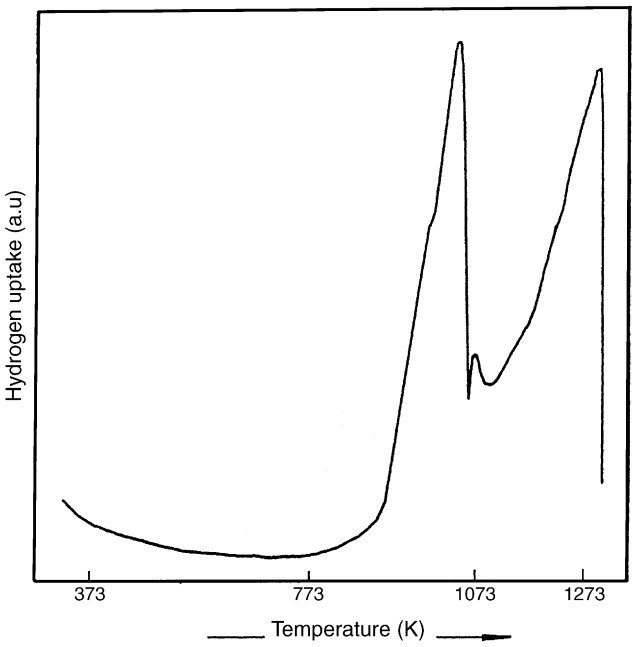


Fig. 5. Temperature-programmed reduction (TPR) profile of pure $MoO_3$.

The sharp peak at 1040 K corresponds to the reduction of $MoO_3$ (first step) and the peak at 1270 K is associated with the reduction of the second step. A minor peak at the edge of the first peak is observed at 1070 K, which corresponds to $Mo_4O_{11}$ formed by reduction of $MoO_3$. Thomas [37] also noticed this peak during TPR of $MoO_3$ and confirmed it by in situ XRD:

$$MoO_3 \rightarrow Mo_4O_{11}$$

Temperature-programmed reduction profiles of $V_2O_5/ZrO_2$ and $MoO_3$–$V_2O_5/ZrO_2$ catalysts are shown in Fig. 6. The dependence of $T_{max}$ values on the $MoO_3$ content are shown in Table 2. The TPR of $V_2O_5/ZrO_2$ show a single peak with $T_{max}$ at 751 K, which is attributed to the reduction of $V^{4+}$. These results are in agreement with the results of Koranne et al. [33], where in they found a single major reduction peak above 773 K in the TPR of $V_2O_5/Al_2O_3$. The results of TPR of various $MoO_3$–$V_2O_5/ZrO_2$ catalysts show a systematic change in the reduction of vanadia with the increase of molybdena promoter. The TPR profiles for all samples have shown two prominent maxima ($T_{max}$) and their position are listed in Table 2. The low temperature peak in the region of 790 K is due to the reduction of $V^{5+}$ to $V^{4+}$. The $T_{max}$ increased with the addition of molybdenum oxide and it is higher than that of $V_2O_5/ZrO_2$ (Table 2). The reduction temperature shifted to higher values (751–795 K) as the molybdena loading was increased from 0.5 to 4 wt.%, suggesting an increase in particle size of microcrystalline vanadia. This shows the decrease in the dispersion of vanadia on zirconia support and which is also evidenced from oxygen chemisorption measurements. The second major peak appeared above 1190 K in all $MoO_3$–$V_2O_5/ZrO_2$ catalysts is due to the reduction of $MoO_3$. The intensity of second peak due to molybdena

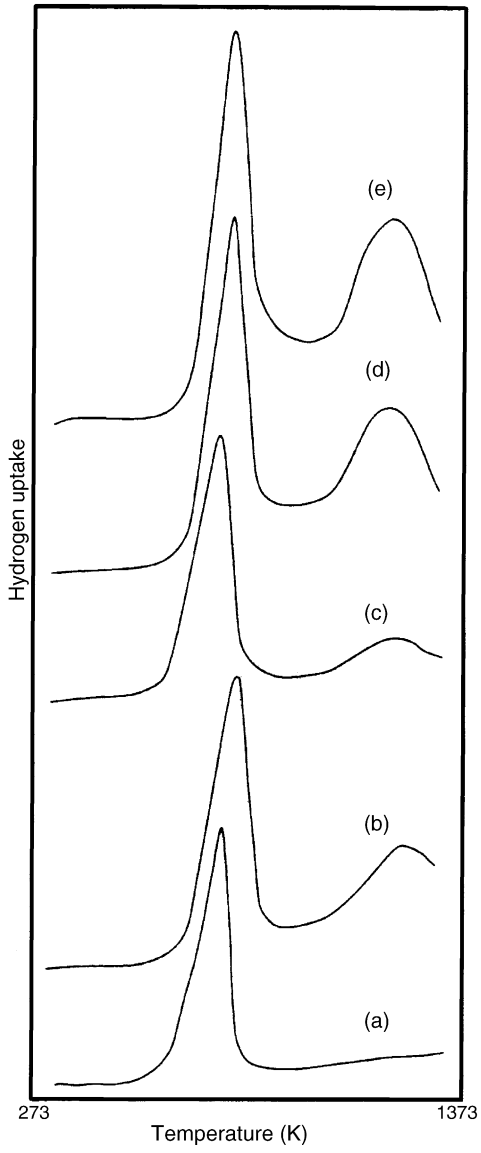


Fig. 6. TPR profiles of $MoO_3$–$V_2O_5/ZrO_2$ catalysts: (a) 6% $V_2O_5/ZrO_2$; (b) 0.5% $MoO_3$–$V_2O_5/ZrO_2$; (c) 2%; (d) 3%; (e) 4%.

Table 2
TPR results of $MoO_3$–$V_2O_5/ZrO_2$ catalysts

| Catalyst | Wt.% of $MoO_3$ | $T^1_{max}$ (K) | $H_2$ consumption (ml/g) | $T^2_{max}$ (K) | $H_2$ consumption (ml/g) |
|---|---|---|---|---|---|
| 6% VZr | 0 | 751 | 50.5 | – | – |
| 1MoVZr | 0.5 | 790 | 52.0 | 1203 | 10.0 |
| 2MoVZr | 2 | 766 | 46.6 | 1215 | 6.9 |
| 3MoVZr | 3 | 795 | 52.6 | 1199 | 26.2 |
| 4MoVZr | 4 | 795 | 57.3 | 1195 | 36.1 |

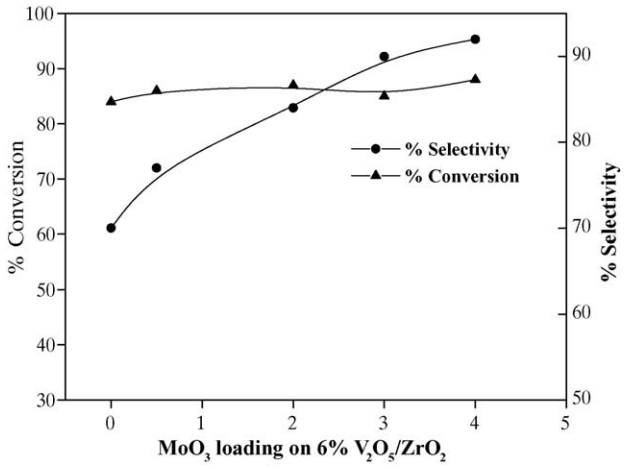


Fig. 7. Ammoxidation of 3-picoline over $MoO_3$–$V_2O_5/ZrO_2$ catalysts.

reduction can be clearly seen with increase in molybdena loading (Fig. 6). The TPR results of $MoO_3$–$V_2O_5/ZrO_2$ catalysts are in agreement with the $H_2$-TPR work of Casagrande et al. [38].

The dependence of $MoO_3$ loading on $V_2O_5/ZrO_2$ catalysts on the conversion and selectivity during the ammoxidation of 3-picoline is shown in Fig. 7. The conversion of 3-picoline was found to be independent of molybdena content in the $V_2O_5/ZrO_2$ catalyst. The conversion did not change much with molybdena addition as a promoter. However, the selectivity of nicotinonitrile formation was found to be increase with increase in molybdena loading. The increase of nicotinonitrile selectivity with $MoO_3$ content might be due to the promotion by Mo species. Our earlier reports [19] also investigate similar activity results on $MoO_3$–$V_2O_5/Al_2O_3$ catalysts during the partial oxidation of methanol. The formaldehyde selectivity was found to increase with $MoO_3$ content on $V_2O_5/Al_2O_3$ system. Molybdenum containing catalysts display a high selectivity in various oxidation reactions: lattice oxide ions are the key reaction participants at temperatures >600 K, while gaseous oxygen reoxidizes the catalysts [39–41]. Since Mars and Van Krevelen [42] first suggested the important role of lattice oxide ions in the selective oxidation of hydrocarbons over metal-oxide catalysts, many studies have been made in this field. The oxide ions resulting from chemisorption and dissociation of the gaseous oxygen on the catalyst surface diffuse through the bulk of the catalyst to the active site at which adsorption and oxidation of the hydrocarbon occur. The following points are elucidated for the surface active sites of $V_2O_5$ catalysts by the effect of $MoO_3$ as a promoter [43]: (i) the surface concentration of redox sites is increased by addition of $MoO_3$ to $V_2O_5$ catalysts. The surface V=O species are newly formed on the various crystal planes of solid solution under the surface Mo=O species on the intermediate compounds are activated under the effect of $V_2O_5$ to act as the redox sites. (ii) The acid sites of $V_2O_5$ catalysts are not modified significantly by the addition of $MoO_3$. The high activity of $V_2O_5$–$MoO_3$ catalysts reported in the literature may be attributed to the increase in the surface concentration of the V=O species on solid solution.

## 4. Conclusions

The effect of molybdenum oxide promoter on 6 wt.% $V_2O_5/ZrO_2$ catalyst is quite significant during the ammoxidation of 3-picoline. The dispersion of vanadia was found to decrease with the addition of molybdena. The oxygen chemisorption results further support the reducibility of catalysts by TPR. XRD results showed the phase transfer changes with the addition of molybdena and which might be due to the specific interactions between vanadia and zirconia support. The catalytic activity during the ammoxidation of 3-picoline reaction does not change much with the addition of molybdena as a promoter. However, it favors the selectivity improvement of nicotinonitrile during ammoxidation.

## References

[1] G.C. Bond, S. Flamerz Tahir, Appl. Catal. 71 (1) (1991), and references therein.
[2] F. Cavani, F. Trifiro, Catal. Today 51 (1999) 561.
[3] I.E. Waches, B.M. Weckhuysen, Appl. Catal. A: Gen. 157 (1997) 91.
[4] K.V.R. Chary, G. Kishan, T. Bhaskar, J. Phys. Chem. 102 (1998) 6792.
[5] P. Forzatti, Appl. Catal. A: Gen. 222 (2001) 221.
[6] F. Roozeboom, T. Fransen, P. Mars, P.J. Gellings, Z. Anorg, Allg. Chem. 449 (1979) 25.
[7] K.V.R. Chary, B. Rama Rao, V.S. Subrahmanyam, Appl. Catal. 74 (1991) 1.
[8] H. Miyata, S. Tokuda, T. Ono, T. Ohno, F. Hatayama, J. Chem. Soc. Faraday Trans. 86 (1990) 2291.
[9] B.M. Reddy, K.V.R. Chary, B. Rama Rao, V.S. Subrahmanyam, C.S. Sunandana, N.K. Nag, Polyhedron 5 (1986) 191.
[10] K.V.R. Chary, K. Ramesh, G. Vidya Sagar, V. Venkat Rao, J. Mol. Cat. A: Chem. 198 (2003) 195.
[11] S. Naito, M. Tsuji, T. Miyao, Catal. Today 77 (2002) 161.
[12] D. Kulkarni, I.E. Waches, Appl. Catal. A: Gen. 237 (2002) 121.
[13] L.J. Burcham, I.E. Wachs, Catal. Today 49 (1999) 467.
[14] R.A. Koppel, C. Stocker, A. Baiker, J. Catal. 179 (1998) 515.
[15] C. Schild, A. Baiker, J. Mol. Catal. 63 (1990) 243.
[16] G. Deo, I.E. Wachs, J. Catal. 146 (1994) 335.
[17] J. Zhu, B. Robenstrof, S.L.T. Andersson, J. Chem. Soc. Faraday Trans. 85 (1989) 3645.
[18] A. Satsuma, F. Okada, A. Hattori, A. Miyamoto, T. Hattori, Y. Murakami, Appl. Catal. 72 (1991) 295.
[19] K.V.R. Chary, V. Venkat Rao, G. Muralidhar, P. Kanta Rao, Catal. Lett. 7 (1990) 389.
[20] M. Najbar, J. Chem. Soc. Faraday Trans. 82 (1986) 1673.
[21] A. Bielanski, M. Najbar, Appl. Catal. A: Gen. 157 (1997) 223.
[22] A. Dejoz, J.M. Lopez Nieto, F. Marquez, M.I. Vazquez, Appl. Catal. A: Gen. 180 (1999) 83.
[23] K.V.R. Chary, G. Kishan, J. Phys. Chem. 99 (1995) 14424.
[24] F. Roozeboom, T. Fransen, P. Mars, P.J. Gellings, Z. Anorg, Allg. Chem. 449 (1979) 25.
[25] S.T. Oyama, G.T. Went, K.B. Lewis, A.T. Bell, G.A. Somorjai, J. Phys. Chem. 93 (1989) 6786.
[26] B.S. Parekh, S.W. Weller, J. Catal. 40 (1987) 100.
[27] F.E. Massoth, G. Muralidhar, J. Shabtai, J. Catal. 85 (1984) 53.
[28] B.S. Parekh, S.W. Weller, J. Catal. 47 (1977) 100.
[29] N.K. Nag, K.V.R. Chary, B.M. Reddy, B. Rama Rao, V.S. Subrahmanyam, Appl. Catal. 9 (1984) 225.
[30] G. Busca, J.C. Lavalley, Spectrochim. Acta 424 (1986) 443.
[31] D. Arco, M. Martin, C. Ramis, G. Busca, V. Lorenzelli, J. Chem. Soc. Faraday Trans. 89 (7) (1993) 1071.
[32] G.C. Bond, A. Sarkani, G.D. Parfitt, J. Catal. 57 (1979) 476.
[33] M. Koranne, J.G. Goodwin, G. Marcelin, J. Catal. 148 (1994) 369.

[34] H. Bosch, B.J. Kip, J.G. van Ommen, P.J. Gellings, J. Chem. Soc. Faraday Trans. I 80 (1984) 2479.
[35] R. Thomas, V.H.J. de Beer, J.A. Moulijn, Bull. Chim. Belg. 90 (1981) 12.
[36] P. Arnoldy, J.C.M. de Jonge, J.A. Moulijn, J. Phys. Chem. 89 (1985) 4517.
[37] R. Thomas, PhD Thesis, University of Amsterdam, 1981.
[38] L. Casagrande, L. Lietti, I. Nova, P. Forzatti, A. Baiker, Appl. Catal. B: Environ. 22 (1999) 63.
[39] G.W. Keulks, J. Catal. 19 (1970) 232.
[40] I. Matsuura, G.C.A. Schuit, J. Catal. 20 (1971) 19.
[41] W. Ueda, Y. Moro-Oka, T. Ikawa, J. Chem. Soc. Faraday Trans. 1 (78) (1982) 495.
[42] P. Mars, D.W. Van Krevelen, Chem. Eng. Sci. Suppl. 3 (1954) 41.
[43] A. Satsuma, A. Hattori, K. Mizutami, A. Furuta, A. Miyamoto, T. Hattori, Y. Murakami, J. Phys. Chem. 93 (1989) 1484.